ATMOSPHERIC SCIENCE

Archean kerogen as a new tracer of atmospheric evolution: Implications for dating the widespread nature of early life

David V. Bekaert,[1]* Michael W. Broadley,[1] Frédéric Delarue,[2] Guillaume Avice,[3] Francois Robert,[2] Bernard Marty[1]

Understanding the composition of the Archean atmosphere is vital for unraveling the origin of volatiles and the environmental conditions that led to the development of life. The isotopic composition of xenon in the Archean atmosphere has evolved through time by mass-dependent fractionation from a precursor comprising cometary and solar/chondritic contributions (referred to as U-Xe). Evaluating the composition of the Archean atmosphere is challenging because limited amounts of atmospheric gas are trapped within minerals during their formation. We show that organic matter, known to be efficient at preserving large quantities of noble gases, can be used as a new archive of atmospheric noble gases. Xe isotopes in a kerogen isolated from the 3.0–billion year–old Farrel Quartzite (Pilbara Craton, Western Australia) are mass fractionated by 9.8 ± 2.1 per mil (‰) (2σ) per atomic mass unit, in line with a progressive evolution toward modern atmospheric values. Archean atmospheric Xe signatures in kerogens open a new avenue for following the evolution of atmospheric composition through time. The degree of mass fractionation of Xe isotopes relative to the modern atmosphere can provide a time stamp for dating Archean kerogens and therefore narrowing the time window for the diversification of early life during the Archean eon.

INTRODUCTION

Because the noble gases are chemically inert, they can yield important insights into the physical processes that affected Earth's atmosphere over geological periods of time. The Xe isotope composition of the Archean atmosphere has been shown to have evolved through geological periods of time toward the modern atmosphere (*1*, *2*). Xe trapped in barite and in fluid inclusions in hydrothermal quartz of Archean ages present Xe isotopic ratios intermediate between modern atmospheric Xe and planetary precursors, showing that atmospheric evolution as a result of mass-dependent fractionation (MDF) was a protracted process still ongoing during the Archean eon [see the study of Avice *et al.* (*2*) and references therein]. However, the limited amounts of ancient atmosphere trapped and preserved in minerals during formation make resolving ancient atmospheric signatures difficult. Carbon-rich lithologies are enriched in heavy noble gases compared to air and seem to be particularly retentive for Xe even at high temperatures (>600°C) (*3*, *4*). Isotopic analyses of large quantities of atmospheric gas possibly contained in organic materials recovered from Archean aged host rocks could potentially allow better constraints on the isotopic composition of atmospheric Xe during the Archean, providing that the organic matter can be shown to be syngenetic [see the study of Avice *et al.* (*2*) and references therein]. Comparing the measured degree of Xe MDF with the value predicted by atmospheric Xe isotope evolution at the time of host rock formation could provide a method to test the syngenetic origin of ancient organic materials.

Earth's atmosphere likely underwent massive escape as the result of giant asteroid impacts (*5*). Primary atmospheric volatiles may therefore have been erased so that Earth's volatile element inventory was largely supplied by late chondritic/cometary deliveries (*6*). From the analysis of fluid inclusions in Archean quartz [Barberton, South Africa, 3.3 billion years (Gy)], the precursor of the modern terrestrial atmosphere has been confirmed as being similar to the U-Xe signature (*2*). U-Xe was initially defined as a theoretical primordial component (*1*), which was required to explain the deficit in heavy Xe isotopes when modern atmospheric Xe is corrected for MDF and compared to solar or chondritic signatures. U-Xe is similar to the solar composition for $^{124–132}$Xe isotopes but exhibits significant depletions of the heavy ^{134,136}Xe isotopes (*1*). Although chondritic and solar compositions are linked by MDF, the U-Xe component appears to be related to a reservoir that is nucleosynthetically different from solar/chondritic compositions. The occurrence of the U-Xe signature in the primitive terrestrial atmosphere (*1*, *6*) is at odds with the chondritic signatures identified for Xe (*7*) and Kr (*8*) in Earth's mantle, which would have been inherited during Earth's main stages of formation. However, the origin of the U-Xe signature in the primitive atmosphere has been recently unraveled in light of the first measurement of the isotopic composition of Xe in a comet by Rosetta spacecraft (*6*). The isotopic composition of cometary Xe shows a deficit in the heavy ^{134,136}Xe isotopes relative to solar Xe and allows the primordial atmospheric component to be computed as a mixture between pure cometary Xe (~20%) and a chondritic (or solar) component (~80%) (*6*).

Remnants of cometary contributions to Earth's inventory during the last phases of terrestrial accretion (referred to as the late accretion episodes) may also be preserved at the present-day lunar surface (*9*). Note that alternative models have been proposed regarding the origin of U-Xe. The primary terrestrial atmosphere has been proposed to have been enriched in ^{134}Xe and ^{136}Xe due to ejection of these isotopes from plutonium/uranium-rich lithologies during fission of the now-extinct ^{244}Pu [chemical fractionation fission process (*10*)]. A giant impact event, such as the one proposed to have formed the Moon, could then have induced major loss of this primary atmosphere, leaving a remaining Xe component that was complimentarily depleted in ^{134}Xe and ^{136}Xe isotopes. However, the time elapsed between Earth's accretion

[1]Centre de Recherches Pétrographiques et Géochimiques, CNRS, Université de Lorraine, UMR 7358, 15 rue Notre Dame des Pauvres, BP 20, 54501 Vandoeuvre-lès-Nancy, France. [2]Institut de Minéralogie, de Physique des Matériaux et de Cosmochimie, Sorbonne Universités—Muséum National d'Histoire Naturelle, Université Pierre et Marie Curie, Université Paris 06, UMR CNRS 7590, IRD UMR 206, Paris, France. [3]Division of Geological and Planetary Sciences, California Institute of Technology, 1200 East California Boulevard, Pasadena, CA 91125, USA.
*Corresponding author. Email: dbekaert@crpg.cnrs-nancy.fr

and the hypothesized giant impact [that is, 30 to 100 million years after the formation of the solar system (*5*)] would be insufficient to allow the accumulation of ^{134}Xe and ^{136}Xe in a primary atmosphere required to account for the subsequent ^{134,136}Xe depletion observed in U-Xe relative to solar/chondritic compositions.

The MDF of U-Xe toward modern atmospheric values is likely to have resulted from Xe escape to space, a process that can also account for the depletion of Xe in air relative to other noble gases [the so-called missing Xe problem (*2*, *11*)]. Thus, the atmosphere became progressively depleted in Xe, relative to the abundance pattern defined by lighter noble gases, and mass dependently fractionated [both properties of atmospheric Xe being referred to as the Xe paradox (*2*)]. In contrast, other atmospheric noble gases were not affected (Ne and Ar) or little affected (Kr), indicating that this escape was Xe-specific. Because Xe is more easily ionized than other noble gases (and other atmospheric species such as CO_2 and N_2), it has been proposed that only processes involving ionization, such as the interaction of the atmosphere with solar ultraviolet light, could have played a role (*2*, *11*, *12*). Ionized Xe would have been dragged away via ionic coupling with escaping H^+ (*12*), thus resulting in the observed long-term evolution of atmospheric Xe (*2*, *11*).

Because they constitute a significant reservoir for atmospheric Xe, carbon-rich lithologies and shales were also proposed as potential carriers of the missing atmospheric Xe (*13*). Bernatowicz *et al.* (*14*) experimentally demonstrated that Xe trapping in sedimentary rocks could account qualitatively, but not quantitatively, for the missing atmospheric Xe. Organic materials trapped within Archean aged rocks therefore potentially record Archean atmospheric signatures retained since formation. However, the processes by which organic materials were produced in Archean environments have not achieved consensus. Several mechanisms including life-related synthesis (*15*), photochemistry and prebiotic synthesis in the atmosphere (*11*, *16*), and geological activity and hydrothermalism (*17*) could have formed organic materials on primitive Earth. Kerogens, that is, chemically isolated insoluble organic matter (IOM), are generally considered to correspond to the sedimentary biological organic matter entrapped in silicified sediments. Investigations about the elemental (H/C and N/C ratios used as a proxy of organic matter preservation) and isotopic composition (δ^{13}C used to track autotrophic metabolism such as photosynthesis) of Archean kerogens provide information on the effect of thermal alteration and/or on the evolution of early life (*18*–*21*). Therefore, the pristine nature of kerogens may represent a mixture of other organic materials originating from secondary hydrothermalism (*17*), from endolithic bacteria (*22*), and/or from modern contamination occurring during sampling (*23*). Because of this multiplicity of potential organic sources, the syngenecity of Archean isolated kerogen and their host rock may not be warranted, thus resulting in ages of the kerogens being potentially decoupled from the geological age of the host rock. Novel criterion is then required to guarantee accurate dating of organic material retrieved from Archean rocks.

Here, we investigate the possible occurrence of trapped ancient atmospheric Ar, Kr, and Xe in a kerogen isolated from black chert originating from the 3.0-Gy-old Farrel Quartzite (Farrel formation, Pilbara Craton, Western Australia). The analysis of multiple new and novel Archean organic kerogens has the potential to trace the temporal evolution of Xe isotopic signatures in the early atmosphere. In this case, the evolution curve of atmospheric Xe isotopes could provide a new tool for confirming an Archean origin for organic samples, thus providing independent age constraints on the development and widespread nature of early life.

RESULTS

Raman spectroscopy

The MGTKS3 kerogen was isolated from a black chert layer originating from the 3.0-Gy-old Farrel Quartzite (Pilbara Craton, Western Australia) and analyzed by Raman spectroscopy in the spectral window from 1000 to 1900 cm^{-1} (see Materials and Methods for details concerning kerogen isolation and Raman spectroscopy). Raman spectra determined on in situ organic matter from the siliceous main matrix and on related kerogen exhibit the same line profile (Fig. 1). These Raman spectra are characterized by the occurrence of the defect (D; ca. 1350 cm^{-1}) and graphite (G; ca. 1600 cm^{-1}) bands, representative of thermally altered kerogens (*24*). Raman line shapes suggest that the MGTKS3 IOM underwent a maximum temperature peak metamorphism of ~350°C (±50°C), in line with the greenschist facies metamorphism that has affected the Farrel Quartzite (*15*). Note that microscopic observations show that organic clots are missing within secondary micro-hydrothermal veins. In accordance, Raman spectroscopy performed on secondary micro-hydrothermal veins does not reveal the existence of carbonaceous matter (Fig. 1), thus precluding any postdeposition contamination and suggesting that studied kerogen consists of syngenetic organic material from the siliceous matrix.

Noble gas analysis

The two aliquots of sample MGTKS3 measured in this study (~6 mg each) yielded identical results. Significant amounts of Ar (1.8×10^{-12} mol ^{36}Ar.g^{-1}), Kr (~4.5×10^{-13} mol ^{84}Kr.g^{-1}), and Xe (5.0×10^{-14} mol ^{130}Xe.g^{-1}) were extracted from the kerogen isolated from the MGTKS3 black chert sample (tables S1 to S3). This corresponds to a ^{130}Xe enrichment

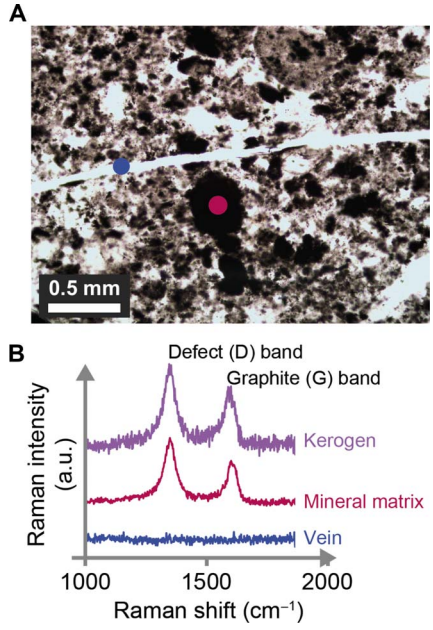

Fig. 1. Raman spectra determined on the kerogen isolated from the black chert sample, on the mineral matrix, and on the secondary hydrothermal veins. (**A**) Transmitted light photography showing that organic matter particles are present in the main mineral matrix but virtually absent in secondary hydrothermal veins. (**B**) Raman spectra determined on the mineral matrix and on the kerogen suggest that the kerogen mostly comprises organic matter from the main mineral matrix. No organic feature is detected in secondary hydrothermal veins. a.u., arbitrary unit.

factor (f) of 250 relative to $^{130}Xe/^{36}Ar$ of air [$f = (([^{130}Xe]/[^{36}Ar])_{sample}/([^{130}Xe]/[^{36}Ar])_{ATM}$], in agreement with the Xe enrichment factors observed in sedimentary rocks (*4*). Argon isotopes reveal an excess contribution of radiogenic ^{40}Ar, with a $^{40}Ar/^{36}Ar$ ratio reaching 2300 [$^{40}Ar/^{36}Ar_{ATM}$: 298.6 (*25*); table S3]. The Kr isotopes are similar to modern atmosphere (Fig. 2 and table S2). All the isotopic spectra of Xe trapped in the kerogen isolated from MGTKS3 consistently exhibit excesses of the light isotopes ($^{124–129}Xe$) together with depletions of heavy isotopes ($^{131–136}Xe$) relative to the modern atmosphere (Fig. 2). We selected the Xe isotope spectrum with the highest deviations from modern atmosphere [9.8 ± 2.1 per mil (‰) per atomic mass unit (amu) at 2σ, 500°C extraction step] as the most representative signature of the trapped component, that is, the one with the least contribution from the modern atmospheric component (Fig. 3). Isotopic fractionation of Xe was computed by error-weighted correlations following the same procedure as that of Avice *et al.* (*2*), that is, by using the stable, nonfissiogenic, non-radiogenic $^{126,128,130}Xe$ isotopes, in addition to ^{131}Xe [only negligibly contributed by the fission of ^{238}U (*26*)]. The red dashed line on Fig. 2 corresponds to the isotopic fractionation of U-Xe relative to modern air [−41.8‰ amu^{-1}; (*1*)]. To derive the isotopic composition of Xe from Barberton Quartz (Fig. 2) (*2*), multiple crushing experiments on several grams of quartz samples were required. The average Xe concentration of each sample was 8.6×10^{-17} mol $^{130}Xe.g^{-1}$. About 580 times more Xe was trapped in the kerogen MGTKS3. This allowed a precision of ≤8‰ (2σ) on average over all the Xe stable isotopes (Fig. 2) to be reached by stepwise heating of a few milligrams of Archean kerogen.

Deviations from the MDF line are in agreement with observed isotopic spectra of Xe retained in Archean fluid inclusions of Barberton quartz (*2*). Monoisotopic depletions of ^{129}Xe and large excesses of the heaviest isotopes relative to the mass fractionation trends are detected in both spectra (Fig. 2). Once corrected for mass fractionation relative to U-Xe, the $^{131–136}Xe$ excesses are fully compatible with the presence of products of the spontaneous fission of ^{238}U (fig. S1). Xe isotopes extracted from the comparatively recent organic materials yielded Xe isotopic compositions indistinguishable from the modern atmospheric composition (Fig. 2 and table S1).

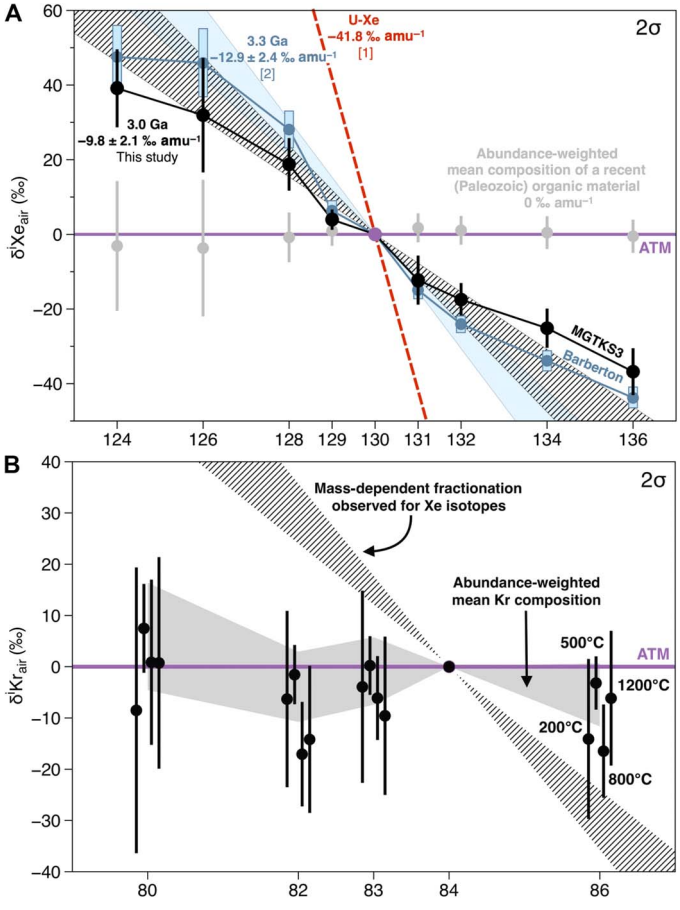

Fig. 2. Isotopic composition of Xe and Kr in the kerogen of the MGTKS3 black chert. The sample is shown relative to the isotopic composition of the modern atmosphere (*25*) and expressed using the δ notation $\delta^{i}Xe_{air} = ((^{i}Xe/^{130}Xe)_{ker}/(^{i}Xe/^{130}Xe)_{air} - 1)*1000$. (**A**) The isotope spectrum of Xe in Barberton quartz samples (3.3 Gy) from Avice *et al.* (*2*), the mass fractionation line of U-Xe (*1*), and the isotopic composition of Xe in a comparatively recent organic material (here the anthracite sample; table S1) are given for comparison. The error envelopes of the MGTKS3 kerogen and Barberton quartz mass fractionation lines are given at 2σ. No mass-dependent isotopic fractionation of Xe isotopes is observed for a recent organic material (table S1). (**B**) The MDF line derived from Xe data is reported for comparison. The abundance-weighted mean composition of Kr in the kerogen of the MGTKS3 black chert sample is essentially atmospheric. Errors are 2σ.

DISCUSSION

Ancient atmospheric Xe in kerogens

This study provides new evidence that the suspected evolution of Xe isotopes in the terrestrial atmosphere has been a global, continuous, and protracted process. Xe trapped in the MGTKS3 kerogen is mass dependently fractionated by −9.8 ± 2.1‰ amu^{-1} (2σ) relative to modern atmospheric Xe (Figs. 2A and 3). Because Xe isotopes extracted from the younger kerogens yielded Xe isotopic compositions similar to those of the modern atmosphere, it is unlikely that Xe MDF occurred during the sample's heating and gas extraction. Because the trapping of Xe atoms in organics does not yield measurable isotopic fractionation without ionization (*27*), Xe isotope fractionation likely did not occur during precipitation of the black chert. In addition, trapping onto solids would favor the heavy isotopes (*27*) and not the light ones as observed here.

The isotopic composition of trapped Kr is similar to that of the modern atmosphere. If Xe isotopes were to have been fractionated during thermal alteration going up to greenschist facies metamorphism, Kr isotopes should also be fractionated to the same extent (or more for a mass-dependent process), which is not observed (Fig. 2). In addition, Raman spectra of the MGTKS3 kerogen suggest that the sample underwent a maximum temperature peak metamorphism of ~350°C, whereas the temperature of main release of the Archean trapped component is around 500°C (Fig. 3). This suggests that the thermal metamorphism experienced by the sample did not significantly affect the trapped Xe component, although the effect of prolonged heating within the geological environment on Xe retention is ultimately unknown. The relative enrichment in light $^{124–129}Xe$ isotopes, together with depletions of heavy $^{131–136}Xe$ isotopes relative to the modern atmosphere, is typically attributed to an Archean atmospheric signature (*2*). These observations indicate that an ancient atmospheric component is likely to have been efficiently trapped and preserved in the MGTKS3 Archean kerogen over geological periods of time. This opens a new avenue for analyzing the past atmosphere by using kerogens as an archive of atmospheric noble gases.

Trapping and preservation of Xe atoms in kerogens

The preservation of atmospheric Xe records in organic materials requires efficient trapping mechanisms. Differences in adsorption coefficients of

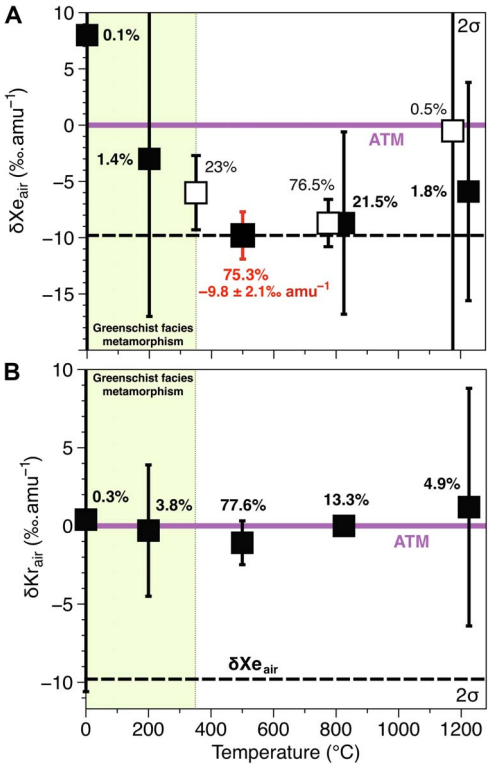

Fig. 3. Degree of mass fractionation (‰ amu^{-1}) of Xe and Kr isotopes isolated from the MGTKS3 black chert kerogen. Degrees of MDF are given for each temperature step relative to the isotopic composition of the modern atmosphere (*25*). The fractions of ^{130}Xe (**A**) and ^{84}Kr (**B**) released for each extraction step relative to the total amount of ^{130}Xe and ^{84}Kr extracted from each aliquot, respectively, are given in percentage. Both series of Xe analysis are shown, with the first and second series represented by open and closed symbols, respectively. Percentage of total gas released during each heating step is displayed beside the symbols. The Xe isotope spectrum with the highest deviations from modern atmosphere (9.8 ± 2.1‰ amu^{-1}, 500°C) is taken as being the most representative signature of the trapped component. This trapped component dominates the budget of Xe isotopes in the sample because more than 75% of the total amount of ^{130}Xe is extracted at this temperature. Errors are 2σ.

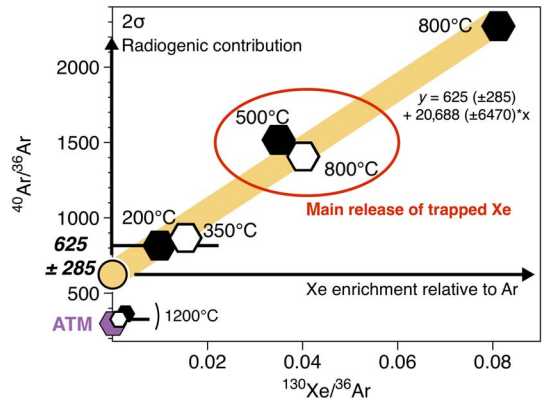

Fig. 4. Mixing diagram of the ^{40}Ar/^{36}Ar ratios as a function of the ^{130}Xe/^{36}Ar ratios. The two series of experiments are represented in open and solid symbols, respectively. The linear trend depicted over stepwise heating of the kerogen isolated from the MGTKS3 black chert sample indicates that the initial ^{40}Ar/^{36}Ar of the fluid [625 ± 285 (2σ)] was higher than the Archean atmospheric ^{40}Ar/^{36}Ar ratio of 143.6 ± 48 (2σ) (*36*), thus confirming that the initial fluid had an excess of radiogenic ^{40}Ar*, possibly related to interaction with crustal and/or hydrothermal reservoirs.

noble gases on activated charcoals [$\alpha_{Xe} \sim 30^{*}\alpha_{Ar}$ at room temperature (*28*)] are unlikely to account for the Xe enrichments relative to Ar observed in sedimentary rocks (*4*). Specific trapping mechanisms are thus required to explain ^{130}Xe enrichment factors relative to ^{36}Ar and to air as observed in our sample ($f = 250$). Several models have been proposed for the strong retention of Xe atoms within organics. Adsorption onto surface-associated defects could account for unusually high retention of heavy noble gases (*29*). This has been experimentally demonstrated to occur for several natural samples, including minerals (*9*, *30*, *31*). The heavy noble gases that are thus "irreversibly adsorbed" onto carbonaceous matter can only be removed by heating the samples at medium to high temperatures (up to 700°C) (*31*), making the process of anomalous adsorption different from common physisorption due to van der Waals forces. In addition, strong retention of Xe in organic materials may be caused by the presence of labyrinth-with-constrictions (*31*) or single-walled nanotube structures (*32*), causing an enhanced adsorption of Xe by electron shell interactions with carbon atoms. Both processes involve an active discrimination of Xe with respect to small atoms due to restricted pathway radii, on the order of the atomic radius. Additional mechanisms may be related to the presence of dangling functional groups (for example, −COOH) inside Xe diffusion paths (*33*), which would delay/prevent Xe mobility within the organic matrix. During the sample's carbonization [first grade of thermal alteration (*24*)], the structural changes of the carbonaceous matter result in structural units of nanometer-sized polyaromatic layers that, coupled to the effect of polyaromatic layer stacking, would drastically reduce the porosity of the sample. In addition to the effect of thermal alteration on organic matter features, the achievement of a closed system during silicification and the very low diffusion coefficients for Xe resulting from its large radius probably contribute together to the preservation of the trapped Xe component in Archean kerogen over geological periods of time.

The syngenecity of organic material cracking before 350°C is highly disputable because it can originate from several postdeposition contaminations (*34*) and/or from residual bitumen (soluble fraction of organic matter) for which syngenecity is still an open issue (*23*). In turn, the Xe-trapped component related to these thermolabile organic materials could not be considered as syngenetic. Thermal cracking of syngenetic Archean stricto sensu kerogens occurs at higher temperature. For instance, Spangenberg and Frimmel (*35*) demonstrated that late Archean organic matter cracked at about 450°C. Thus, the release of Archean Xe in the range of 400° to 600°C should be closely related to the cracking of syngenetic and thermorecalcitrant organic material.

Depositional environment

The occurrence of radiogenic ^{40}Ar* (^{40}Ar/^{36}Ar up to 2300) (Fig. 4 and table S3) and fissiogenic $^{131-136}$Xe (fig. S1) produced by the decay of ^{40}K and spontaneous fission of ^{238}U, respectively, suggests that there is a contribution from crustal fluids within the sample. The ^{40}Ar/^{36}Ar ratio can be expressed as a function of ^{130}Xe/^{36}Ar

$$\frac{^{40}\mathrm{Ar}}{^{36}\mathrm{Ar}} = \frac{^{40}\mathrm{Ar}_{\mathrm{init}} + {}^{40}\mathrm{Ar}^{*}}{^{36}\mathrm{Ar}} = \left(\frac{^{40}\mathrm{Ar}}{^{36}\mathrm{Ar}}\right)_{\mathrm{init}} + \left(\frac{^{40}\mathrm{Ar}^{*}}{^{130}\mathrm{Xe}}\right) \mathrm{x} \left(\frac{^{130}\mathrm{Xe}}{^{36}\mathrm{Ar}}\right) \quad (1)$$

where ^{40}Ar$_{init}$ is ^{40}Ar inherited from the fluid that interacted with the kerogen (either at the time of the chert formation or during thermal alteration going up to greenschist facies metamorphism) and ^{40}Ar* is

radiogenic ^{40}Ar produced in situ by the decay of ^{40}K. The linear trend depicted over stepwise heating in a three-isotope diagram of the $^{40}Ar/^{36}Ar$ ratio versus the $^{130}Xe/^{36}Ar$ ratio indicates that the initial $^{40}Ar/^{36}Ar$ ratio of the fluid, given by the *y* intercept of the regression line, was at least 625 ± 285 (2σ) (Fig. 4). This is higher than the Archean atmospheric $^{40}Ar/^{36}Ar$ ratio of 143.6 ± 48 (2σ) (*36*), in line with the occurrence of a fluid presenting radiogenic ^{40}Ar in excess of the atmospheric composition, probably related to interaction with crustal and/or hydrothermal reservoirs. At any temperature step, the $^{130}Xe/^{36}Ar$ ratios up to 8×10^{-2} are higher than the atmospheric ratio [$^{130}Xe/^{36}Ar_{ATM} = 1.13 \times 10^{-4}$ (*25*); Fig. 4], thus revealing a contribution from the Xe-enriched trapped component. Contribution from the modern atmosphere (^{36}Ar) component decreases with increasing temperature steps. The main release of the trapped Xe component occurs at ~500°C (Fig. 3). At higher temperature, the residual gas is dominated by the strongly retained Xe component and by in situ produced radiogenic $^{40}Ar^*$.

The trapped Xe component could have been incorporated in organic materials at the same time as the black chert formation or, alternatively, supplied later by secondary hydrothermal fluids circulating in the continental crust and interacting with the sample during its burial. In both cases, the fluids carrying dissolved Xe are expected to be at isotopic equilibrium with the Archean atmosphere composition, regardless of the possible fissiogenic contributions from their interaction with rocks. In the case of the studied Archean sample, the lack of any postdepositional organic material, as revealed by microscopic observations and Raman spectroscopy, and the high-temperature release of the Xe component suggest that the degree of mass fractionation detected for Xe isotopes corresponds to a pristine Archean signature. Note that the deficit of $^{129}Xe^*$ from the decay of the now-extinct ^{129}I ($T_{1/2}$: 16 Ma) relative to the atmospheric composition (Fig. 2) argues against a contribution from mantle-derived fluids (*2*). The depletion in ^{129}Xe relative to the Xe mass fractionation line likely reflects a lower $^{129}Xe^*$ excess in the Archean atmosphere relative to the present (*2*).

Heavy noble gas escape to space and MDF of a U-Xe–like precursor

As observed in this study, Kr isotopes are not significantly mass fractionated in Archean records compared to modern air [see the study of Avice *et al.* (*2*) and references therein]. This implies that the physical process that drove continuous Xe loss from the atmosphere did not significantly affect lighter noble gases. Because of its low ionization potential relative to Kr, atmospheric Xe would have been readily ionized by ultraviolet radiation from the early Sun before being dragged along open magnetic field lines and lost to space via ionic coupling with escaping H (*12*). Such a process can account for the continuous MDF of Xe isotopes in the atmosphere, whereas Kr isotopes, with a higher ionization potential, would not have been affected. Nonetheless, even if ionized (and lost to space) to a minor extent, MDF of atmospheric Kr isotopes through time is a possibility. To date, no Archean record permitted the atmospheric precursors of Kr to be deciphered [see the study of Avice *et al.* (*2*) and references therein]. The initial Kr isotopic composition of the atmosphere could be chondritic- [Q-Kr; (*37*)] or solar-like (*38*) or could have resulted from a mixture of both components. Kr isotopes extracted at 500°C (>75% release; Fig. 3) show a potential MDF of −1.08 ± 1.40‰ amu^{-1} (2σ), in favor of the light isotopes (Fig. 5). Whereas Q-Kr is depleted in the light isotopes relative to modern air, solar Kr is mass dependently fractionated in favor of the light isotopes, and thus appears to be a better candidate for the precursor atmospheric Kr (Fig. 5), in agreement with the conclusion reached by Holland *et al.* (*8*). Additional analyses of Archean Kr signatures are required to confirm this possibility.

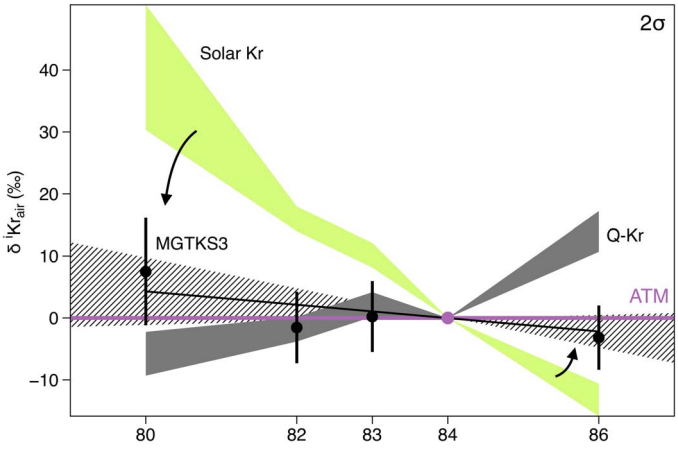

Fig. 5. Isotopic composition of Kr in the kerogen of the MGTKS3 black chert. The sample is shown relative to the isotopic composition of the modern atmosphere (*25*) and expressed using the δ notation $\delta^{i}Kr_{air} = (({}^{i}Kr/{}^{84}Kr)_{ker}/({}^{i}Kr/{}^{84}Kr)_{air} - 1)*1000$. The chondritic krypton [Q-Kr; (*37*)] and solar Kr (*38*) compositions are given for comparison. Whereas Q-Kr is depleted in the light isotopes relative to modern air, solar Kr is mass dependently fractionated in favor of the light isotopes, relative to modern air, and thus appears to be a better candidate for the precursor atmospheric Kr, although additional and repeated analyses of Archean Kr signatures are required to confirm this interpretation.

Dating the blossoming and widespread nature of early life

The earliest evidence of life remains subject to debate (*39*). Because ages of kerogens may potentially be decoupled from the geological age of the host rock, accurately dating organic material retrieved from Archean rocks requires the organic materials to be dated independently. Using Ar-Ar dating is complicated by the potential for the kerogens to be overprinted by the radiogenic contribution from the host rock, inheriting an unknown radiogenic component during formation and/or having K contents affected during the sample's isolation. The light Xe isotope signature in kerogens only relies on the composition of the atmosphere at the time of Xe trapping and does not rely on understanding the chemistry of the sample and host rock. The degree of mass fractionation of Xe trapped in Archean organic materials relative to modern atmosphere therefore provides a potentially new and unique tool for dating microfossil-bearing metasediments.

The MDF of atmospheric Xe with time relative to modern atmosphere can be modeled as a power law ($y = 0.238*x^{3.41}$) fitting the literature data of Xe isotope mass fractionation in ancient samples as well as the initial (U-Xe) and final (modern atmosphere) compositions (Fig. 6 and fig. S2). When reported on the evolution curve of atmospheric Xe, the degree of mass fractionation detected for Xe isotopes (9.8 ± 2.1‰ amu^{-1}, 2σ) provides a model age of 3.0 ± 0.2 Gy (2σ) for the silica-embedded kerogen (Fig. 6). This age for the kerogen MGTKS3 is in excellent agreement with the geological age of the chert [2.95 Gy (*15*)]. From a physical basis, the use of a power law to model Xe isotope evolution in the atmosphere has been classically chosen in the framework of Rayleigh fractionation [for example, in the case of hydrodynamic escape of neutral species (*40*)]. Dauphas (*41*) used a phenomenological model, such as the generalized power law, as a proxy of atmospheric Xe isotope fractionation law. Fundamentally, Xe escape is a function of both solar radiation [extreme ultraviolet (XUV)] from the early Sun (required to

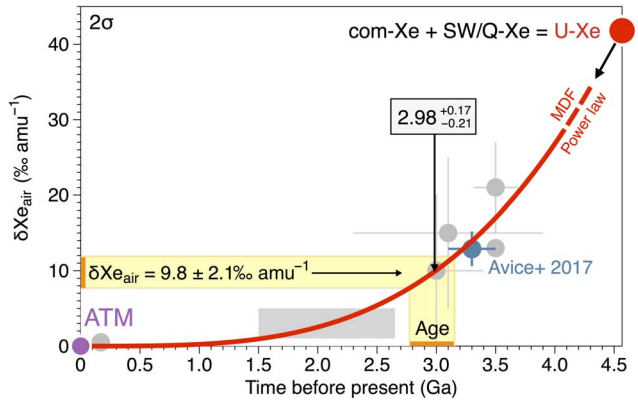

Fig. 6. MDF of atmospheric Xe with time relative to modern atmosphere. The red curve was established from a power law ($y = 0.238*x^{3.41}$) fitting the literature data of Xe isotope mass fractionation in ancient samples [see the study of Avice *et al.* (*2*) and references therein] as well as the initial [U-Xe, the precursor of Earth's atmosphere (*1*)]) and final [modern atmosphere (*25*)] compositions of the atmosphere. Isotopic composition is expressed in per mil per atomic mass unit relative to the modern atmosphere (purple dot) (*25*). The degree of MDF obtained in this study for the kerogen isolated from the MGTKS3 black chert sample (9.8 ± 2.1‰ amu^{-1}, 2σ) can be used to estimate the age of the sample from the evolution curve of the isotopic fractionation of atmospheric Xe. This method would provide a model age of 3.0 ± 0.2 Gy (2σ) for the kerogen embedded in silica, in excellent agreement with the geological age of the chert [2.95 Gy (*15*)].

ionize Xe) and H^+ escaping rate (required to drag Xe) (*12*). Although the evolution of H escape over time is not well constrained, Ribas *et al.* (*42*) found that stellar fluxes can be very well approximated by power-law relationships. Because a linear relation is expected between the hydrogen escape rate and the solar radiation level (*43*), we speculate that the power law that we determine in this study may be related to an effective XUV power law. Our model assumes a continuous and nondisrupted evolution of Xe isotopes in the past atmosphere. This hypothesis remains to be verified at the high-resolution level by multiple analyses of atmospheric Xe isotopes trapped in ancient samples.

This method should also be applied on a case-by-case basis, taking into account the geological history of each sample. Multiple sources of postdepositional carbonaceous materials (*17*), mass fractionation effects during the sample's maturation and/or partial filling/emptying of the sample's porosity by secondary fluid circulations (*4*), as well as metamorphism and reset processes (*44*) could all possibly alter the trapped Xe component over geological time scales. In the absence—or limit—of this potential bias, any apparent age given by this method should be seen as a minimal age because the trapped composition is expected to reflect the last chemical equilibration between the kerogen and the atmosphere (possibly air or air-saturated fluids).

The Great Oxygenation Event that occurred about 2.3 Ga (*45*) thoroughly changed the course of biological evolution. Before the rise of O_2 in the atmosphere, CH_4 was probably an important trace atmospheric constituent that contributed to the greenhouse effect, balancing the lower luminosity of the early Sun (*46*). Extensive H loss during the Archean constitutes an alternative to organic burial for removing photosynthetic reductants from the atmosphere and permitting O_2 accumulation. Tracking the evolution of Xe isotopes in the past atmosphere offers a crucial observational basis to constrain hydrogen loss to space and provide information about the timing of Earth surface's irreversible oxidization at the time of life emergence (*45*). Estimates of the gradual changes in the H rate of escape could conceivably yield estimates of H_2 concentrations in early Earth's atmosphere. This information is highly relevant to the origin of life because redox conditions in the atmosphere control the efficiency of prebiotic organic compound production through abiotic Miller-Urey–type synthesis (*16*). Last, note that constraining the extent and timing of atmospheric Xe MDF may provide information about terrestrial planets' paleoclimates. The limited Xe MDF that occurred in the Martian early atmosphere (before 4.2 Ga) suggests that Martian hydrogen escape was not sufficient enough to support long-term MDF of Xe isotopes in the Martian atmosphere and, thus, that limited amounts of liquid water—yielding H_2 by photodissociation—were present on Mars at this period of time (*47*).

CONCLUSION

The large amounts of noble gases preserved in organic matter, when compared to fluids trapped in minerals, unlock a previously untapped reservoir and allow the evolution of atmospheric Xe to be determined with unprecedented resolution. Archean atmospheric Xe signatures in undisturbed kerogens open up new horizons for analyzing the past atmosphere. This study presents new evidence that atmospheric Xe was progressively enriched in heavy isotopes and depleted in light isotopes during the Archean eon. Precise heating steps permit modern versus ancient atmosphere to be distinguished and should help to constrain the mechanisms of noble gases trapping in organic materials. Noble gases can be used as powerful tools to provide information about the depositional environment of organic materials at the time of life diversification. The degree of mass fractionation relative to modern atmosphere can provide a model age for dating the last chemical equilibration between the organic matter and the atmosphere.

MATERIALS AND METHODS

Samples

The MGTKS3 black chert sample was collected from the ca. 3.0-Gy-old Farrel Quartzite at the Mount Grant locality in the Goldsworthy greenstone belt, Pilbara Craton, Western Australia. The Farrel Quartzite is composed of a clastic formation up to 80 m thick containing fine- to very coarse–grained sandstone, including quartzite with minor conglomerate, mafic to ultramafic volcanoclastic layers, evaporite beds, and black chert layers (*15*). This unit underwent greenschist facies metamorphism and was pervasively silicified (*15*, *24*). The ca. 30-cm-thick microfossil-bearing black chert occurs in the uppermost part of the Farrel Quartzite and is closely associated with evaporite beds.

Two Paleozoic—so comparatively younger—natural organic materials were also analyzed for their Xe isotope composition following the same analytical protocol: a type III kerogen from Champclauson (Gard, France; Stephanian, Upper Carboniferous) and an anthracite sample from La Motte-d'Aveillans (Isère, France; Upper Carboniferous). These two samples were selected to test whether geologically younger organic materials would yield modern atmospheric Xe isotope compositions.

IOM isolation from the MGTKS3 black chert sample

The MGTKS3 kerogen was isolated through successive demineralization of ca. 200 g of black chert using HF-HCl treatments at room temperature (*24*). Soluble organic compounds were first removed by stirring powdered cherts in dichloromethane/methanol (2/1, v/v). Carbonates were then dissolved using hydrochloric acid (HCl; 37%). Samples were then centrifuged and washed with distilled water until reaching neutrality. The concentration of the kerogen was achieved by acid maceration

at room temperature in a mixture of HF (40%) and HCl (37%) acids (2:1, v/v). Samples were again centrifuged and washed with distilled water. Neoformed fluorides were degraded using HCl (37%) at 60°C (24 hours). Finally, the kerogen was centrifuged/washed with distilled water before being dried through successive steps of acetone rinsing and evaporation.

Raman spectroscopy

Raman spectra were obtained using a Renishaw inVia microspectrometer, equipped with a 532-nm argon laser. The laser was focused on the sample using a DMLM Leica microscope with a 50× lens. The spectrometer was first calibrated with a silicon standard before the analytical session (*24*). For each target, we determined the Raman shift intensity in the spectral window from 1000 to 1900 cm^{-1} including the first-order disorder carbon (D) and graphite (G) bands. Spectra acquisition was achieved after two successive iterations using a time exposure of 40 s. A laser power below 1 mW was used to prevent any thermal alteration during the spectra acquisition.

Noble gas analysis

Ar, Kr, and Xe were extracted from the kerogen by step heating using a filament furnace (*48*). The furnace consists of four alumina-coated tungsten evaporation baskets (Ted Pella Inc.) welded to a pair of nickel rods mounted on eight-pin electrical feedthrough flange. Temperatures were estimated by using foils of pure metals with known melting points (tin, 230°C; aluminum, 660°C; copper, 1085°C; and nickel, 1455°C) and were controlled during heating steps by direct measurement using an optical pyrometer. Before loading the samples, each basket was degassed at ~1600°C to remove any adsorbed atmospheric noble gases. The samples were wrapped in tantalum foil and loaded into the baskets before baking the entire furnace at >150°C overnight under high vacuum. Samples were loaded individually to avoid indirect heating and degassing of other samples during analysis. Kerogen MGTKS3 (12 mg in total) was split into two aliquots (~6 mg each). The first aliquot was heated over three temperature steps (~350°, ~800°, and ~1200°C), and only Ar and Xe isotopes were measured. The second aliquot was heated over four temperature steps (~200°, ~500°, ~800°, and ~1200°C), with Kr isotopes being measured in addition to Ar and Xe.

Gases released during step heating were first purified on an in-line Ti-sponge getter heated to 600°C to remove any active species. Kr and Xe were then condensed onto a quartz tube at liquid nitrogen temperatures for 20 min. The remaining Ar in the preparation line was then expanded to a further series of Ti-sponge getters, three at 550°C and one at room temperature for a further 20 min to remove any final reactive species. The Ar fraction was expanded into the spectrometer (Helix MC Plus, Thermo Fisher Scientific) and analyzed using peak jumping mode on faraday (^{40}Ar) and compact dynode multiplier ($^{36,38}Ar$) collectors. After Ar analysis, any remaining gas was pumped. To remove the remaining Ar trapped within the quartz tube, three dilutions from the glass tube (20 cm^3) to the whole line (1500 cm^3) in static mode were made to reduce the partial pressure of Ar. Kr and Xe gas fractions were then released from the tube at room temperature and purified on getters following the same protocol as Ar. Both Kr and Xe were simultaneously expanded into the spectrometer and analyzed using the compact dynode multiplier, with Xe isotopes being measured first, followed by the measurement of Kr isotopes. Blanks were measured at the same temperature as the samples using a basket loaded with empty tantalum foil packets. Blanks at 500°C, the temperature at which most of the gas from the samples was released, were 2.4×10^{-13} mol ^{40}Ar, 8.6×10^{-17} mol ^{84}Kr, and 1.2×10^{-18} mol ^{130}Xe. These amounts correspond to <3% of the ^{40}Ar and ^{84}Kr and <1% of the ^{130}Xe released from the sample, making blank corrections minimal. Note that our calibration standard for the Kr is not well calibrated, so Kr abundances are only indicative, although the Kr isotope compositions are accurate. Error propagation for Ar, Kr, and Xe isotopic analyses is detailed in Appendix B of Bekaert *et al.* (*9*).

SUPPLEMENTARY MATERIALS

Supplementary material for this article is available at http://advances.sciencemag.org/cgi/content/full/4/2/eaar2091/DC1

table S1. Xe isotopic composition of the kerogen isolated from the MGTKS3 black chert sample and from two Paleozoic—so comparatively younger—kerogens (an anthracite and a type III kerogen called Champclauson) by stepwise heating.

table S2. Kr isotopic composition of the kerogen isolated from the MGTKS3 black chert sample by stepwise heating.

table S3. Ar isotopic composition of the kerogen isolated from the MGTKS3 black chert sample by stepwise heating.

fig. S1. Fission spectrum of MGTKS3 kerogen Xe corrected for mass fractionation relative to U-Xe.

fig. S2. Comparison of power law/exponential law fit of the literature data [see the study of Avice *et al.* (*2*) and references therein] on the evolution of atmosphere Xe isotope fractionation over geological periods of time.

REFERENCES AND NOTES

1. R. O. Pepin, On the origin and early evolution of terrestrial planet atmospheres and meteoritic volatiles. *Icarus* **92**, 2–79 (1991).
2. G. Avice, B. Marty, R. Burgess, The origin and degassing history of the Earth's atmosphere revealed by Archean xenon. *Nat. Commun.* **8**, 15455 (2017).
3. U. Frick, S. Chang, Ancient carbon and noble gas fractionation. *Proc. Lunar Sci. Conf.* **8**, 263–272 (1977).
4. T. Torgersen, B. M. Kennedy, M. C. van Soest, Diffusive separation of noble gases and noble gas abundance patterns in sedimentary rocks. *Earth Planet. Sci. Lett.* **226**, 477–489 (2004).
5. K. Zahnle, L. Schaefer, B. Fegley, Earth's earliest atmospheres. *Cold Spring Harb. Perspect. Biol.* **2**, a004895 (2010).
6. B. Marty, K. Altwegg, H. Balsiger, A. Bar-Nun, D. V. Bekaert, J.-J. Berthelier, A. Bieler, C. Briois, U. Calmonte, M. Combi, J. De Keyser, B. Fiethe, S. A. Fuselier, S. Gasc, T. I. Gombosi, K. C. Hansen, M. Hässig, A. Jäckel, E. Kopp, A. Korth, L. Le Roy, U. Mall, O. Mousis, T. Owen, H. Rème, M. Rubin, T. Sémon, C.-Y. Tzou, J. H. Waite, P. Wurz, Xenon isotopes in 67P/Churyumov-Gerasimenko show that comets contributed to Earth's atmosphere. *Science* **356**, 1069–1072 (2017).
7. A. Caracausi, G. Avice, P. G. Burnard, E. Füri, B. Marty, Chondritic xenon in the Earth's mantle. *Nature* **533**, 82–85 (2016).
8. G. Holland, M. Cassidy, C. J. Ballentine, Meteorite Kr in Earth's mantle suggests a late accretionary source for the atmosphere. *Science* **326**, 1522–1525 (2009).
9. D. V. Bekaert, G. Avice, B. Marty, B. Henderson, M. S. Gudipati, Stepwise heating of lunar anorthosites 60025, 60215, 65315 possibly reveals an indigenous noble gas component on the Moon. *Geochim. Cosmochim. Acta* **218**, 114–131 (2017).
10. A. P. Meshik, O. V. Pravdivtseva, C. M. Hohenberg, New evidence for chemical fractionation of radioactive xenon precursors in fission chains. *Phys. Rev. C* **93**, 044614 (2016).
11. E. Hébrard, B. Marty, Coupled noble gas–hydrocarbon evolution of the early Earth atmosphere upon solar UV irradiation. *Earth Planet. Sci. Lett.* **385**, 40–48 (2014).
12. K. J. Zahnle, Xenon fractionation and Archean hydrogen escape, *46th Lunar and Planetary Science Conference*, The Woodlands, TX, 16 to 20 March, 2015.
13. F. A. Podosek, M. Honda, M. Ozima, Sedimentary noble gases. *Geochimica et Cosmochimica Acta*, **44**, 1875–1884 (1980).
14. T. J. Bernatowicz, F. A. Podosek, M. Honda, F. E. Kramer, The atmospheric inventory of xenon and noble gases in shales: The plastic bag experiment. *J. Geophys. Res. Solid Earth* **89**, 4597–4611 (1984).
15. K. Sugitani, K. Grey, A. Allwood, T. Nagaoka, K. Mimura, M. Minami, C. P. Marshall, M. J. Van Kranendonk, M. R. Walter, Diverse microstructures from Archaean chert from the Mount Goldsworthy–Mount Grant area, Pilbara Craton, Western Australia: Microfossils, dubiofossils, or pseudofossils? *Precambrian Res.* **158**, 228–262 (2007).
16. S. L. Miller, G. Schlesinger, Carbon and energy yields in prebiotic syntheses using atmospheres containing CH_4, CO and CO_2. *Orig. Life* **14**, 83–90 (1984).
17. A. O. Marshall, J. R. Emry, C. P. Marshall, Multiple generations of carbon in the Apex chert and implications for preservation of microfossils. *Astrobiology* **12**, 160–166 (2012).

18. Y. Watanabe, H. Naraoka, D. J. Wronkiewicz, K. C. Condie, H. Ohmoto, Carbon, nitrogen, and sulfur geochemistry of Archean and Proterozoic shales from the Kaapvaal Craton, South Africa. *Geochim. Cosmochim. Acta* **61**, 3441–3459 (1997).
19. J. L. Eigenbrode, K. H. Freeman, Late Archean rise of aerobic microbial ecosystems. *Proc. Natl. Acad. Sci. U.S.A.* **103**, 15759–15764 (2006).
20. C. P. Marshall, G. D. Love, C. E. Snape, A. C. Hill, A. C. Allwood, M. R. Walter, M. J. Van Kranendonk, S. A. Bowden, S. P. Sylva, R. E. Summons, Structural characterization of kerogen in 3.4 Ga Archaean cherts from the Pilbara Craton, Western Australia. *Precambrian Res.* **155**, 1–23 (2007).
21. D. Frédéric, R. François, S. Kenichiro, T. Romain, D. Rémi, D. Sylvie, Investigation of the geochemical preservation of *ca*. 3.0 Ga permineralized and encapsulated microfossils by nanoscale secondary ion mass spectrometry. *Astrobiology* **17**, 1192–1202 (2017).
22. T. R. R. Bontognali, A. L. Sessions, A. C. Allwood, W. W. Fischer, J. P. Grotzinger, R. E. Summons, J. M. Eiler, Sulfur isotopes of organic matter preserved in 3.45-billion-year-old stromatolites reveal microbial metabolism. *Proc. Natl. Acad. Sci. U.S.A.* **109**, 15146–15151 (2012).
23. K. L. French, C. Hallmann, J. M. Hope, P. L. Schoon, J. A. Zumberge, Y. Hoshino, C. A. Peters, S. C. George, G. D. Love, J. J. Brocks, R. Buick, R. E. Summons, Reappraisal of hydrocarbon biomarkers in Archean rocks. *Proc. Natl. Acad. Sci. U.S.A.* **112**, 5915–5920 (2015).
24. F. Delarue, J. N. Rouzaud, S. Derenne, M. Bourbin, F. Westall, B. Kremer, K. Sugitani, D. Deldicque, F. Robert, The Raman-derived carbonization continuum: A tool to select the best preserved molecular structures in Archean kerogens. *Astrobiology* **16**, 407–417 (2016).
25. D. Porcelli, C. J. Ballentine, R. Wieler, An overview of noble gas geochemistry and cosmochemistry. *Rev. Mineral. Geochem.* **47**, 1–19 (2002).
26. R. A. Ragettli, E. H. Hebeda, P. Signer, R. Wieler, Uranium-xenon chronology: Precise determination of λ_{sf*} $^{136}Y_{sf}$ for spontaneous fission of ^{238}U. *Earth Planet. Sci. Lett.* **128**, 653–670 (1994).
27. Y. Marrocchi, B. Marty, Experimental determination of the xenon isotopic fractionation during adsorption. *Geophys. Res. Lett.* **40**, 4165–4170 (2013).
28. S. Dushman, *Scientific Foundations of Vacuum Technique* (John Wiley & Sons, 1957), 806 pp.
29. Y. Marrocchi, B. Marty, P. Reinhardt, F. Robert, Adsorption of xenon ions onto defects in organic surfaces: Implications for the origin and the nature of organics in primitive meteorites. *Geochim. Cosmochim. Acta* **75**, 6255–6266 (2011).
30. J. Yang, R. S. Lewis, E. Anders, Sorption of noble gases by solids, with reference to meteorites. I: Magnetite and carbon. *Geochim. Cosmochim. Acta* **46**, 841–860 (1982).
31. J. F. Wacker, M. G. Zadnik, E. Anders, Laboratory simulation of meteoritic noble gases. I. Sorption of xenon on carbon: Trapping experiments. *Geochim. Cosmochim. Acta* **49**, 1035–1048 (1985).
32. V. Simonyan, J. K. Johnson, A. Kuznetsova, J. T. Yates Jr., Molecular simulation of xenon adsorption on single walled carbon nanotubes. *J. Chem. Phys.* **114**, 4180–4185 (2001).
33. A. Kuznetsova, J. T. Yates Jr., J. Liu, R. E. Smalley, Physical observation of xenon in open single walled carbon nanotubes: Observation of a quasi-one-dimensional confined Xe phase. *J. Chem. Phys.* **112**, 9590–9598 (2000).
34. S. Derenne, F. Robert, A. Skrzypczak-Bonduelle, D. Gourier, L. Binet, J.-N. Rouzaud, Molecular evidence for life in the 3.5 billion year old Warrawoona chert. *Earth Planet. Sci. Lett.* **272**, 476–480 (2008).
35. J. E. Spangenberg, H. E. Frimmel, Basin-internal derivation of hydrocarbons in the Witwatersrand Basin, South Africa: Evidence from bulk and molecular δ^{13} C data. *Chem. Geol.* **173**, 339–355 (2001).
36. M. Pujol, B. Marty, R. Burgess, G. Turner, P. Philippot, Argon isotopic composition of Archaean atmosphere probes early Earth geodynamics. *Nature* **498**, 87–90 (2013).
37. H. Busemann, H. Baur, R. Wieler, Primordial noble gases in "phase Q" in carbonaceous and ordinary chondrites studied by closed-system stepped etching. *Meteorit. Planet. Sci.* **35**, 949–973 (2000).
38. A. Meshik, C. Hohenberg, O. Pravdivtseva, D. Burnett, Heavy noble gases in solar wind delivered by Genesis mission. *Geochim. Cosmochim. Acta* **127**, 326–347 (2014).
39. M. A. van Zuilen, A. Lepland, G. Arrhenius, Reassessing the evidence for the earliest traces of life. *Nature* **418**, 627–630 (2002).
40. D. M. Hunten, R. O. Pepin, J. C. G. Walker, Mass fractionation in hydrodynamic escape. *Icarus* **69**, 532–549 (1987).
41. N. Dauphas, The dual origin of the terrestrial atmosphere. *Icarus* **165**, 326–339 (2003).
42. I. Ribas, E. F. Guinan, M. Güdel, M. Audard, Evolution of the solar activity over time and effects on planetary atmospheres. I. High-energy irradiances (1–1700 Å). *Astrophys. J.* **622**, 680 (2005).
43. F. Tian, O. B. Toon, A. A. Pavlov, H. De Sterck, A hydrogen-rich early Earth atmosphere. *Science* **308**, 1014–1017 (2005).
44. F. L. Staplin, Sedimentary organic matter, organic metamorphism, and oil and gas occurrence. *Bull. Can. Petrol. Geol.* **17**, 47–66 (1969).
45. D. C. Catling, K. J. Zahnle, C. P. McKay, Biogenic methane, hydrogen escape, and the irreversible oxidation of early Earth. *Science* **293**, 839–843 (2001).
46. A. A. Pavlov, J. F. Kasting, L. L. Brown, K. A. Rages, R. Freedman, Greenhouse warming by CH_4 in the atmosphere of early Earth. *J. Geophys. Res.* **105**, 11981–11990 (2000).
47. W. S. Cassata, Meteorite constraints on Martian atmospheric loss and paleoclimate. *Earth Planet. Sci. Lett.* **479**, 322–329 (2017).
48. R. Burgess, P. Cartigny, D. Harrison, E. Hobson, J. Harris, Volatile composition of microinclusions in diamonds from the Panda kimberlite, Canada: Implications for chemical and isotopic heterogeneity in the mantle. *Geochim. Cosmochim. Acta* **73**, 1779–1794 (2009).

Acknowledgments: We thank L. Zimmermann, Y. Marrocchi, and K. Zahnle for fruitful discussions. We also thank V. Rouchon and O. Belhadj (Center for Research on the Preservation of Collections, USR 3224) for Raman microspectroscopy. **Funding:** This study was supported by the European Research Council (grants PaleoNanoLife 2011-ADG_20110209 to F.R. and PHOTONIS 695618 to B.M.). This is Centre de Recherches Pétrographiques et Géochimiques–CNRS contribution #2549. **Author contributions:** D.V.B. did the noble gas analyses, discussed the results and their interpretations, and wrote the manuscript. M.W.B. participated in the noble gas analyses, discussed the results and their interpretations, and participated in writing the manuscript. F.D. did the IOM isolation from the MGTKS3 black chert sample, performed Raman analyses, discussed the interpretations, and participated in writing the manuscript. G.A., F.R., and B.M. discussed the results and their interpretations and participated in writing the manuscript. **Competing interests:** The authors declare that they have no competing interests. **Data and materials availability:** All data needed to evaluate the conclusions in the paper are present in the paper and/or the Supplementary Materials. Additional data related to this paper may be requested from the authors.

Submitted 16 October 2017
Accepted 30 January 2018
Published 28 February 2018
10.1126/sciadv.aar2091

Citation: D. V. Bekaert, M. W. Broadley, F. Delarue, G. Avice, F. Robert, B. Marty, Archean kerogen as a new tracer of atmospheric evolution: Implications for dating the widespread nature of early life. *Sci. Adv.* **4**, eaar2091 (2018).

Science Advances

Archean kerogen as a new tracer of atmospheric evolution: Implications for dating the widespread nature of early life

David V. Bekaert, Michael W. Broadley, Frédéric Delarue, Guillaume Avice, Francois Robert and Bernard Marty

Sci Adv **4** (2), eaar2091.
DOI: 10.1126/sciadv.aar2091